J Mater Sci: Mater Med (2010) 21:1183–1193
DOI 10.1007/s10856-010-3987-7

Ultrastructural evaluation of in vitro mineralized calcium phosphate phase on surface phosphorylated poly(hydroxy ethyl methacrylate-co-methyl methacrylate)

G. S. Sailaja · P. Ramesh · H. K. Varma

Received: 4 October 2009 / Accepted: 3 January 2010 / Published online: 23 January 2010

Abstract The in vitro functionality of surface phosphorylated poly(hydroxy ethyl methacrylate-co-methyl methacrylate), poly(HEMA-co-MMA) to induce bioinspired mineralization of calcium phosphate phase is evaluated. The primary nucleation of calcium phosphate on the surface phosphorylated copolymer occurs within 3 days of immersion when immersed in 1.5× simulated body fluid and the degree of mineralization is proportional to the hydroxy ethyl methacrylate content in the copolymer. The calcium phosphate phase is identified as hydroxyapatite by X-Ray diffraction analysis. The transmission electron microscopic evaluation combined with selected area diffraction pattern and energy dispersive analysis exemplified that the primary nuclei of amorphous calcium phosphate transforms to crystalline needle like calcium rich apatite, within a period of 3 days immersion in simulated body fluid. The atomic force microscopic results corroborate the c-axis growth of the crystals within 3 days immersion in SBF.

G. S. Sailaja · H. K. Varma (✉)
Bioceramics Lab, Biomedical Technology Wing, Sree Chitra Tirunal Institute for Medical Sciences and Technology, Poojappura, Thiruvananthapuram 695 012, India
e-mail: varma@sctimst.ac.in

G. S. Sailaja
e-mail: sailajags@gmail.com

P. Ramesh
Polymer Processing Laboratory, Biomedical Technology Wing, Sree Chitra Tirunal Institute for Medical Sciences and Technology, Poojappura, Thiruvananthapuram 695 012, India
e-mail: rameshp@sctimst.ac.in

1 Introduction

Surface functionalisation has been employed as a potential technique by various investigators for achieving functional properties such as hydrophilicity, biomolecular recognition, cytocompatibility and bioinspired mineralization [1–4]. Surface functionalisation of polymers with anionic groups, such as phosphate and carboxylate, can persuade interactions with mineral precursor ions and hence extensively investigated for bio-inspired mineralization of calcium phosphate and its epitaxial growth on macromolecular surface under in vitro environment [5–9]. Moreover, surface phosphorylation accomplished greater significance due to its superior potential to induce nucleation of hydroxyapatite [10].

Poly(methyl methacrylate), PMMA bone cement is clinically used for the fixation of hip prostheses [11]. However, in spite of the relatively good success rate of implant fixation with acrylic-based bone cement, the Bone-PMMA bone cement interface is one of the major weak-link zones in the prosthesis-bone cement-bone construct particularly because of the incapability of PMMA to undergo osseointegration [12, 13]. Investigations have proved that calcium phosphate coating on the implant surface can inspire bonding with host bone [14, 15]. Attempts towards imparting biofunctionality to PMMA to achieve this property have been undertaken by various researchers [16–18]. However, most of these research works were attempted towards developing a composite material of PMMA with calcium phosphate or surface functionalization of PMMA followed by a calcium hydroxide pretreatment [16–18]. In a recent study, the authors have reported that surface phosphorylated copolymer of methyl methacrylate, 'poly (hydroxy ethyl methacrylate-co-methyl methacrylate)', poly(HEMA-co-MMA) is capable of promoting direct bone bonding [19]. Here, in this paper, the authors focus on the in

vitro functionality assessment of the surface phosphorylated poly(HEMA-co-MMA) as a function of HEMA content and the ultra-structural evaluation of the primary nuclei formed during mineralization. The surface phosphorylated poly(HEMA-co-MMA) triggered nucleation of calcium phosphate without any pretreatment. The role of HEMA to promote phosphorylation and thereby invoke bioinspired mineralization of calcium phosphate is quantitatively assessed by atomic absorption and UV–Visible spectroscopy. The ultra-structural evaluation of the primary nuclei formed during mineralization has been performed using transmission electron microscopy and atomic force microscopy.

2 Experimental part

2.1 Materials

2-Hydroxy ethyl methacrylate (HEMA) (Assay: 98%), methyl methacrylate (MMA) (Assay: 99%) and phosphorous pentoxide (Assay: 98+, ACS reagent) were procured from Aldrich chemical Co., USA. Ethylene glycol dimethacrylate (EGDMA) (Assay: 98%) was obtained from Fluka, USA. Benzoyl peroxide (Assay: 98%) was purchased from s.d. Fine India Ltd, Mumbai, India. All other chemicals are procured from Ranbaxy India Pvt. Ltd, Mumbai, India.

Methyl methacrylate was made free of inhibitor by treating with 4% sodium hydroxide solution for three times, followed by washing with distilled water and dried by placing over anhydrous magnesium sulphate. HEMA was made free of inhibitor by passing through an inhibitor remover column (Aldrich chemical Co., USA)

2.2 Synthesis of poly(2-HEMA-co-MMA)

Poly(2-hydroxy ethyl methacrylate-co-methyl methacrylate) with HEMA:MMA mole ratio varying as 0.07:0.90, 0.57: 0.25, 0.69: 0.10 (represented as PH1, PH4 and PH5 respectively) were synthesized by free radical initiated bulk polymerization using 0.5 wt% benzoyl peroxide as initiator under nitrogen atmosphere at 80°C and 1-wt% ethylene glycol dimethacrylate as in situ cross-linker.

2.3 Surface phosphorylation of poly(2-HEMA-co-MMA)

The surface phosphorylation of poly(2-HEMA-co-MMA) was performed using 76% phosphorous pentoxide (P_2O_5) at 80°C in a RB flask for 60 min [20]. The films were cooled to room temperature and washed with distilled water. The films were further immersed in deionized water for a period of 72 h with frequent changes of deionized water to make free of excess reagents, and dried in an air oven at 70°C.

2.4 Characterization

Micro FT-IR spectra of the samples were collected using Thermo Nicolet 5700 FT-IR microscope (Madison, WI) in the attenuated total reflectance (ATR) mode. The estimation of the surface bound phosphate per unit area was quantitatively measured using UV–visible spectrophotometer, Shimadzu UV mini –1240 [21].

The in vitro mineralization assessment of the surface functionalized poly(HEMA-co-MMA) was performed using 1.5× simulated body fluid (SBF) as per the procedure reported by Kokubo et al. [22]. The unmodified poly(HEMA-co-MMA), poly(HEMA) and PMMA were used as control samples. The samples were retrieved from SBF after 3, 10 and 15 days, washed with deionized water and dried in an air oven at 50 ± 2°C. The calcium phosphate phase formed was analyzed by wide-angle X-ray diffraction patterns taken using D5005 X-ray diffractometer (SIEMENS, Germany) with scanning angle 2θ, from 5 to 50 and compared with hydroxyapatite PDF data (9-432). The calcium phosphate crystal morphology is viewed using a scanning electron microscope (SEM Hitachi model S-2400, Japan) after gold coating the specimens.

The ultra structural features of the calcium phosphate coating, its transformation from amorphous to crystalline state and the calcium to phosphorous ratio have been observed with the help of a transmission electron microscope,—(Jeol 2000, Japan),—coupled with energy dispersive X-ray detector. The calcium phosphate particles were dispersed in methanol, carefully transferred onto carbon coated copper grid, dried and viewed. The selected area electron diffraction patterns (SAED) of the coating were collected to identify the amorphous to crystalline transformation. The calcium to phosphorous ratio was calculated using the EDS detector attached to the TEM.

The surface topography and roughness profile of PH1, surface phosphorylated PH1 (designated as PPH1) and the finer aspects of the calcium phosphate coating formed on surface phosphorylated PH1 were acquired using atomic force microscope cantilevers (spring constant = 0.58 N/m) in the contact mode using Digital Instruments Multimode Nanoscope E with the software Nanoscope V 6.12 r2. The measurement was performed in the contact mode. The quantitative estimation of calcium in the calcium phosphate coating formed on the surface of phosphorylated PH1 after immersing in 1.5SBF for different time intervals was performed using atomic absorption spectroscopy (Varian spectr AA10 machine, Varian Techtron, Victoria, Australia).

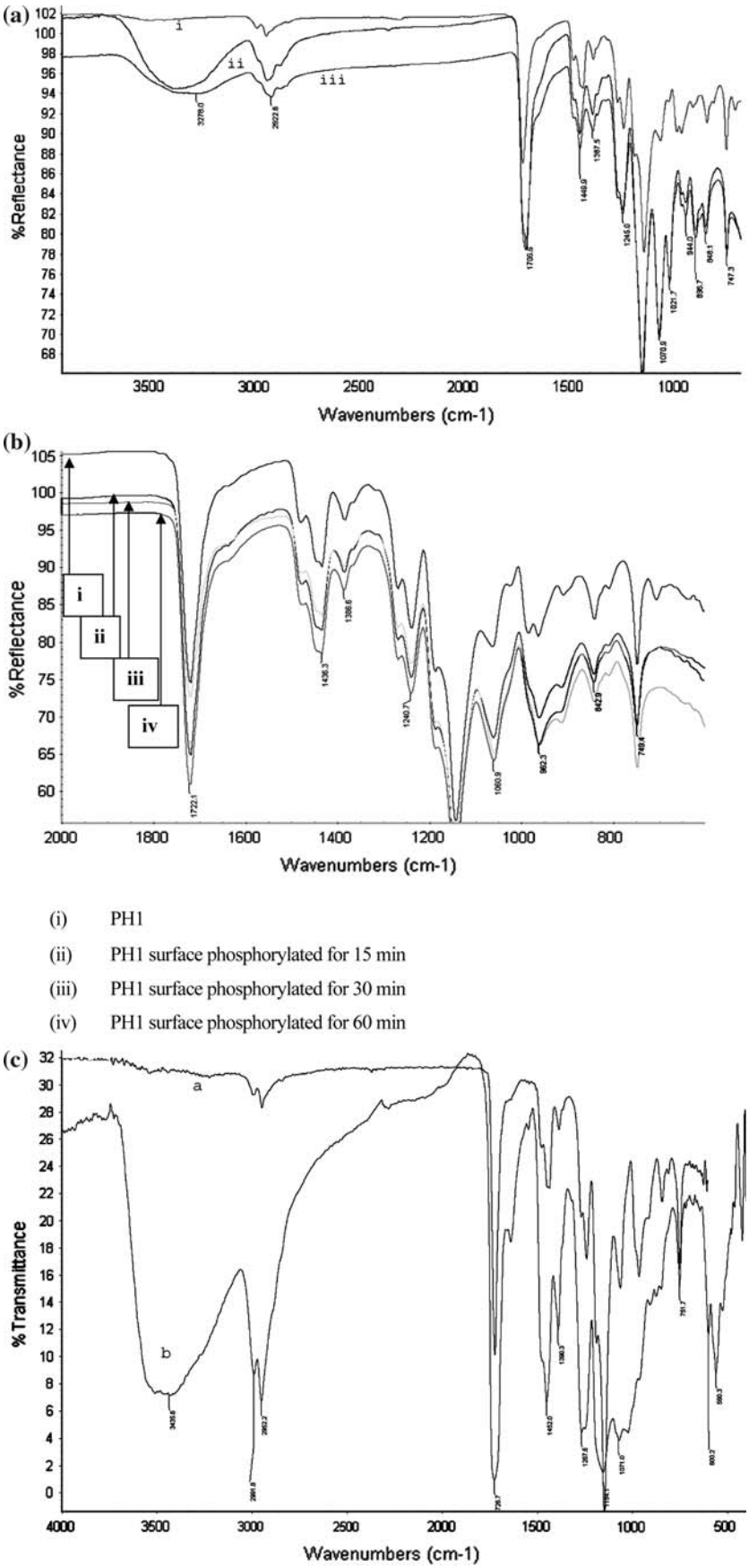

Fig. 1 **a** Micro FT-IR spectra of PH1 (i), PH4 (ii), PH5 (iii). **b** Micro FT-IR spectrum of surface phosphorylated PH1 at different time periods in comparison with PH1. (i) PH1, (ii) PH1 surface phosphorylated for 15 min, (iii) PH1 surface phosphorylated for 30 min, (iv) PH1 surface phosphorylated for 60 min. **c** Micro FT-IR spectrum of PH1 (a) and calcium phosphate coated PH1 (b)

3 Results and discussion

3.1 Micro FT-IR

The ATR spectra of PH1, PH4 and PH5 are shown in Fig. 1a. All the compositions have characteristic –C = O and $–CH_3$ peaks at 1706, 2922 cm^{-1} respectively, while PH4 and PH5 have –OH peak at 3375 cm^{-1}. As the HEMA content in the copolymer increases, the –OH peak becomes prominent in the spectrum.

Figure 1b depicts the micro FT-IR overlay spectrum of phosphorylated PH1, phosphorylated for different time periods in comparison with unmodified PH1. In the spectra, PH1 is compared with PH1 phosphorylated for 15, 30 and 60 min. The surface phsophorylated PH1 series show peaks corresponding to the phosphate group at 1060.9 and 962.3 cm^{-1}.

Figure 1c shows the micro FT-IR specrum of PH1 phosphorylated for 60 min and immersed in 1.5SBF for 3 days. The spectrum imparts clear indications of formation of calcium phosphate coating on PH1 by the presence of new peaks corresponding to inorganic P–O stretching (1154 and 1071 cm^{-1}) and P–O bending (560 cm^{-1}) vibration modes and a broad peak at 3435 cm^{-1} of –OH group.

3.2 UV–Visible spectroscopy

The extent of phosphorylation as a function of HEMA wt% in poly(HEMA-co-MMA) is given in Fig. 2. The phosphate concentration per unit surface area of the phosphorylated copolymer is given in Table 1. It is apparent from the fig that the phosphate concentration increases with increase in HEMA wt% and reaches the highest value for phosphorylated poly(HEMA) showing that the extent of phosphorylation is proportional to HEMA content in poly(HEMA-co-MMA). The surface phosphate concentration is significant even for PPH1 (HEMA: MMA 0.07:0.90) when compared to phosphorylated poly(HEMA).

3.3 Wide angle X-ray diffraction

The X-ray diffractogram of the calcium phosphate coating formed on PPH1 upon 15 days immersion in SBF is shown in Fig. 3. The diffractogram has two broad 2θ peaks at 26° and 31–34° that are typical for a poorly crystalline hydroxyapatite.

3.4 Scanning electron microscopy

The scanning electron micrographs of primary and secondary calcium phosphate nuclei formed on PPH1 at different time periods are shown in Fig. 4a–f. The primary nucleation begins within 3 days immersion in SBF (Fig. 4a, b) and by 10 days, the entire surface is covered by a layer of calcium phosphate, on which secondary nucleation begins (Fig. 4c, d). The propagation of the secondary growth is visible in Fig. 4e and f with unique spheroid morphology. The high magnification images reveal that the spheroid like superstructure of the coating are composed of fine network of tiny apatite crystals with a few void-like appearances. The control samples used for in vitro mineralization study are PH1, PMMA and poly(HEMA), given as Fig. 4g–i, respectively. It could be viewed from the SEM images that calcium phosphate nucleation is absent in control samples.

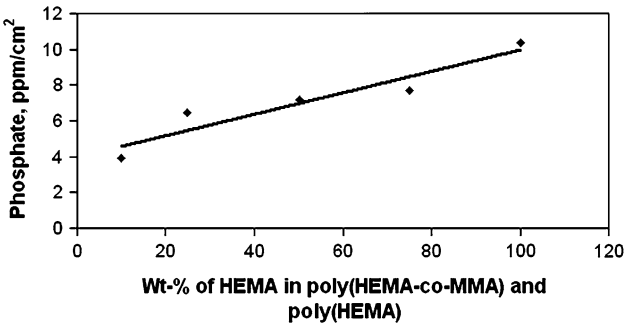

Fig. 2 Phosphate concentration as a function of HEMA wt% in phosphorylated poly(HEMA-co-MMA) and in phosphorylated poly(HEMA)

Table 1 The phosphate concentration as a function of HEMA wt% in phosphorylated poly(HEMA-co-MMA) and in phosphorylated poly(HEMA)

Sample code	Wt% of HEMA in phosphorylated poly(HEMA-co-MMA) series and Poly(HEMA)	Phosphate concentration (ppm/cm^2)
PPH1	10	3.9437
PPH2	25	6.4289
PPH3	50	7.1438
PPH4	75	7.6726
PPH (Poly(HEMA)	100	10.3468

3.5 Transmission electron microscopy and energy dispersive X-ray (TEM-EDS) analysis

The ultra-structural features of the calcium phosphate nuclei formed on surface phosphorylated PH1 immersed in 1.5 SBF for 3 days are revealed in the transmission electron micrograph (Fig. 5a). The transmission electron micrographs show that the spheroid-like apatite clusters found in SEM are composed of needle like apatite rods of 10–12 nm diameter and 70–100 nm length. Another

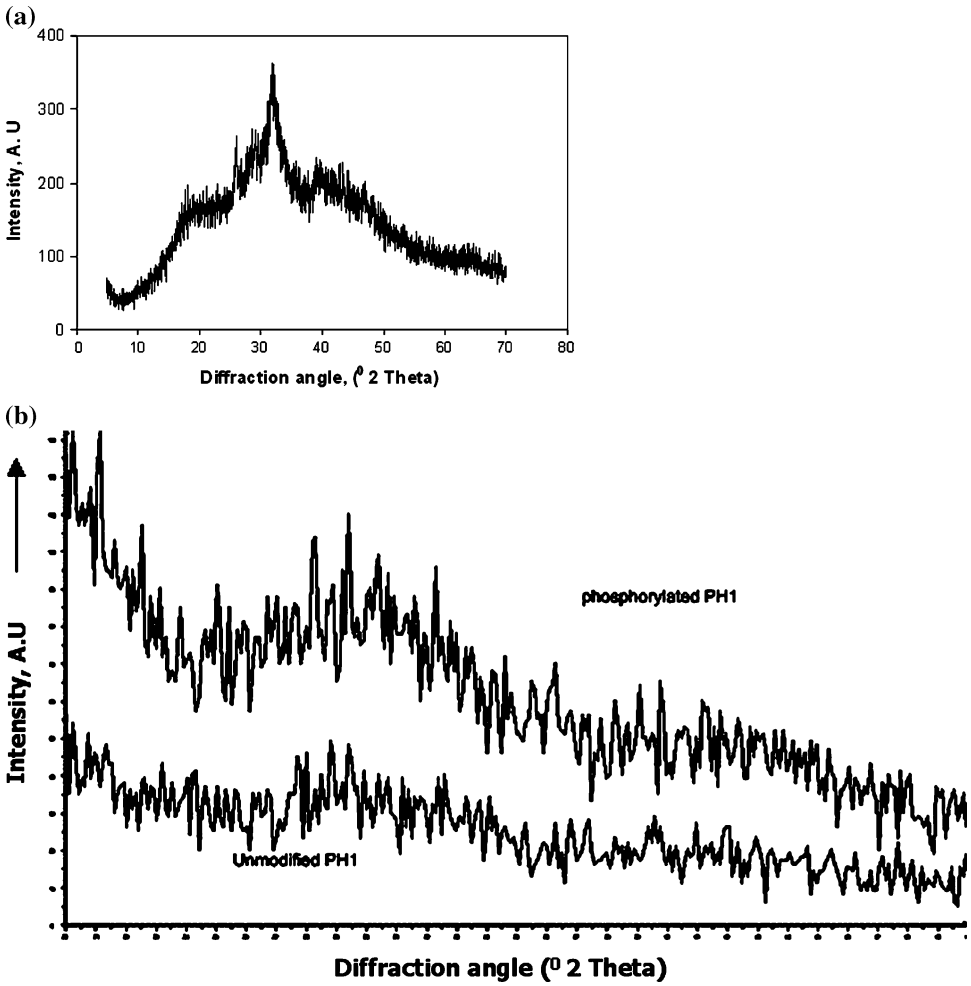

Fig. 3 **a** X-ray diffraction pattern of poorly crystalline apatite coating formed on PPH1 upon 15 days immersion in SBF. **b** X-ray diffraction patterns of unmodified PH1 and phosphorylated PH1

important observation is the transformation of calcium phosphate from amorphous state to crystalline phase begins as early as 3 days immersion in 1.5× SBF as evident from the selected area electron diffraction (SAED) pattern of the crystalline region shown at the inset (Fig. 5a). The EDS spectra of the crystalline and amorphous regions are shown in Fig. 5b and c, respectively showing the presence of calcium rich apatite. The needle like apatite crystals are better viewed in high magnification micrograph (Fig. 5d).

3.6 Atomic force microscopy (AFM)

The atomic force microscopy technique was used to view the surface topography of PH1 and phosphorylated PH1. The AFM images obtained for the samples are compared in Fig. 6a–d. The surface topography of phosphorylated PH1 (Fig. 6c, d) appeared rougher compared to PH1 illustrating that phosphorylation significantly imparts greater roughness to the copolymer surface. The AFM images of phosphorylated PH1 were collected after immersing the samples in 1.5SBF for 3 days. The images were collected in both height and deflection modes, and are given as Fig. 7a and b, respectively. The three dimensional view of the same area is given as Fig. 7c. It is apparent that the crystals are <200 nm in length and <20 nm thick and have a specific growth orientation (Fig. 7b). However, when the samples were immersed in 1.5SBF for longer periods, the crystal size increased to 400–600 nm.

3.7 Atomic absorption spectroscopy (AAS)

The calcium concentration in the calcium phosphate coating deposited on phosphorylated PH1 was estimated as a function of time using atomic absorption spectroscopy. The calcium concentration of the coating/unit area of phosphorylated PH1 after immersing in SBF at different time intervals is given in Table 2. It could be viewed that the concentration of calcium in the coating increases linearly with time of immersion in SBF (Fig. 8a). The concentration calcium in the coating deposited on phosphorylated poly(HEMA-co-MMA) series is compared with that of phosphorylated poly(HEMA) after immersing in SBF for 15 days is given as Fig. 8b. It is apparent from the Fig that that the calcium concentration of the coating increased with

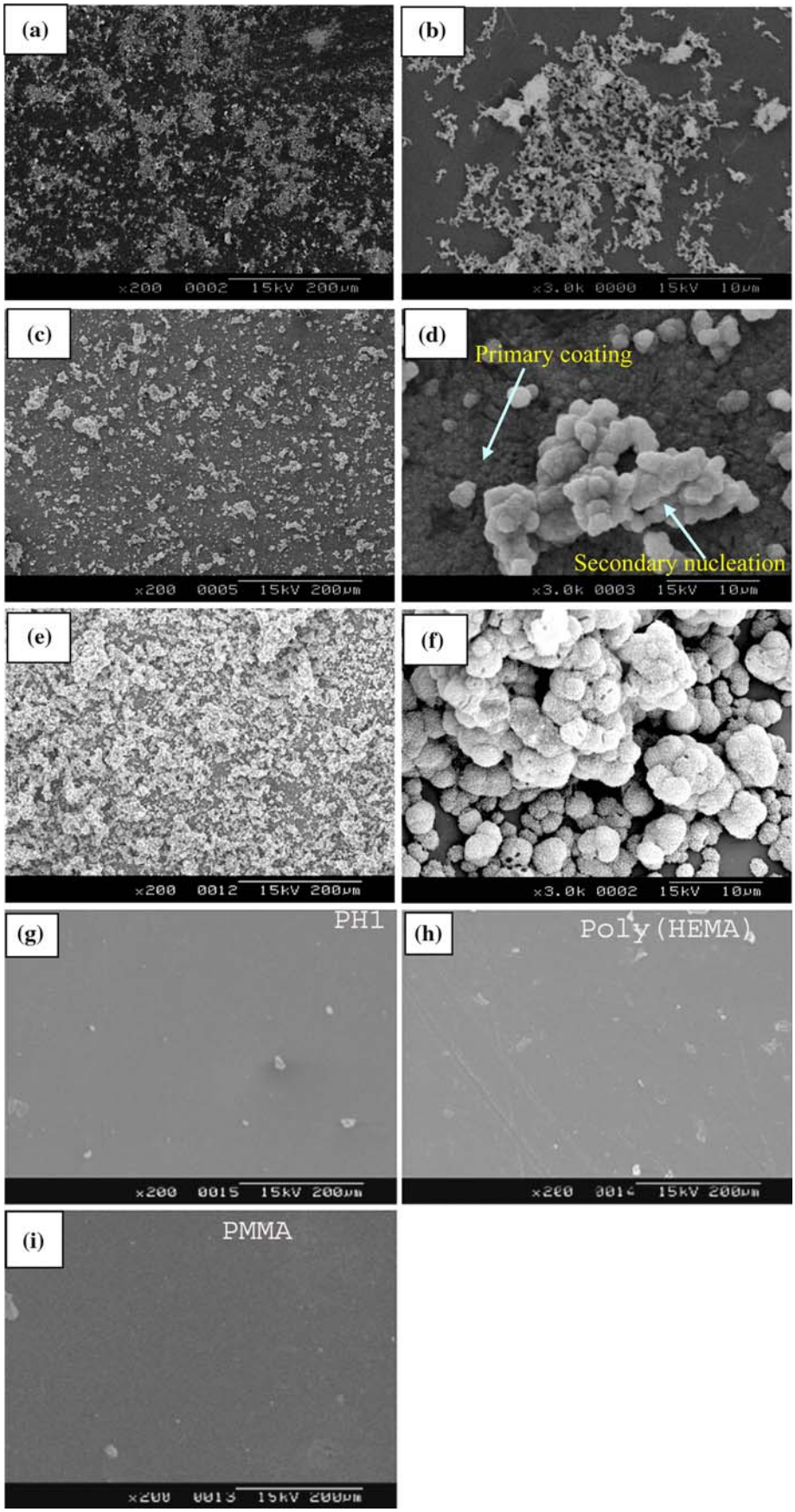

Fig. 4 **a–f** SEM micrographs of (**a**) and (**b**) calcium phosphate coating on PPH1 for 3 days, (**c**) and (**d**) beginning of secondary nucleation at 10 days, (**e**) and (**f**) secondary nucleation completes in 15 days. **g–i** SEM micrographs of control samples PH1, poly(HEMA) and PMMA after immersion in 1.5SBF for 15 days

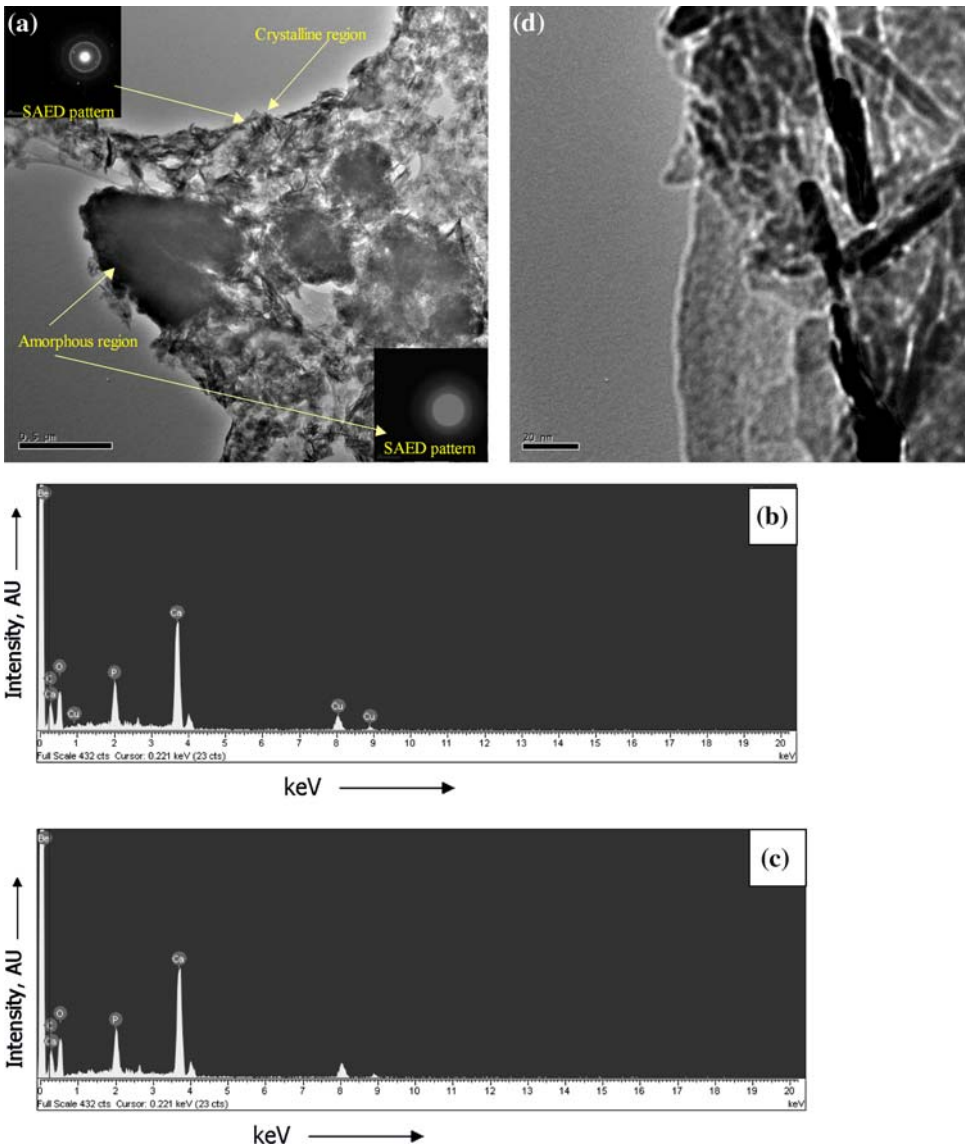

Fig. 5 **a** TEM image of calcium phosphate coating formed on PPH1 upon immersion in SBF for 3 days. **b** Energy dispersive spectrum of crystalline region of the calcium phosphate coating. **c** Energy dispersive spectrum of amorphous region of the calcium phosphate coating. **d** TEM image of needle-like apatite crystals (scale bar = 20 nm)

increase in wt% of HEMA in the phosphorylated PH1 (Fig. 8b). The maximum value was obtained for the surface phosphorylated poly(HEMA) specimens.

4 Discussion

The micro FT-IR spectral analysis confirms the surface phosphorylation of PH1 by the proposed method and the calcium phosphate coated PH1 (Fig. 1c) shows presence of peaks corresponding to –OH, P–O stretching and P–O bending, illustrating the presence of inorganic phosphate group. The UV–Visible spectrometric data show that the extent of phosphorylation is proportional to the HEMA content in poly(HEMA-co-MMA). This could be well correlated to the basic property of poly(HEMA) to undergo reversal of surface structure according to the environment [23]. Hydroxylated polymers exhibit a surface rich in methyl groups (from the polymer chain backbone) in air, and a surface rich in hydroxyl groups in water and thus can undergo a reversal of surface structure when transferred from air into an aqueous environment. [23] It could be assumed that the –OH groups of poly(HEMA-co-MMA) get preferentially exposed to phosphorylating medium and thus actively facilitating the process of surface phosphorylation. Hence it could be proposed that the surface phosphorylation of PH1 with very low HEMA content (HEMA: MMA mole ratio as 0.07:0.90) is principally occurring due to this reason.

It has been reported that the surface energy has a prominent role in triggering crystal nucleation and hence variation in surface topography can also influence surface functional group mediated mineralization [24]. Inorganic crystallization on organic surface primarily occurs by

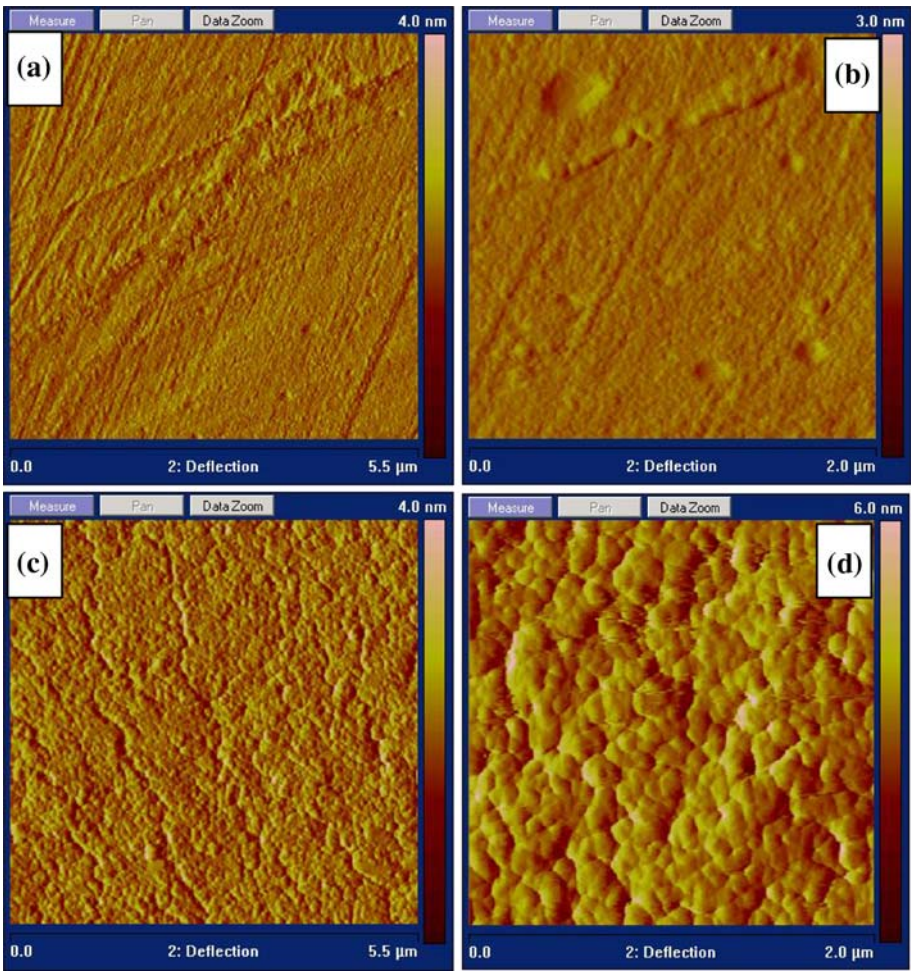

Fig. 6 **a** and **b** Surface topography of PH1, (**c**) and (**d**) Surface topography of PPH1

lowering the activation energy of nucleation [25]. The spatial charge concentration of functional groups on concave surface is higher compared to convex or planar surfaces and thus concave areas could be assumed as surface charge concentrated pockets and has the potential to accelerate crystal nucleation [25]. Hence the topography variation of PH1 as a result of surface phosphorylation is also expected to have a role in facilitating the hydroxyapatite nucleation apart from the anionic surface charge offered by phosphate groups.

The TEM-EDS data clearly indicates the presence of needle-like crystalline calcium phosphate on PPH1 while the AFM data confirm the growth of the crystals in the c-axis. The properties of calcium phosphate crystals formed biomimetically are different from those of biological apatite [26–28]. The apatite crystals deposited by in vitro method are one order of magnitude larger than those of biological apatites [26]. This size variation of biological and in vitro deposited apatite crystals arises due to the differences between in vivo and in vitro crystallization conditions [28]. This implies that the in vivo conditions limit the progressive nucleation stage and three-dimensional growth of apatite crystals. It has already been argued that homogeneous nucleation of particles in the solution will only be dominant at relatively higher levels of supersaturation where the precipitation process becomes kinetically controlled [29]. While, the formation of the inorganic phase directly on a substrate (i.e., heterogeneous nucleation) is the dominant precipitation mechanism for thermodynamically controlled systems.

Kim et al. found that on immersion in SBF, the synthetic HAP is found to induce the formation of bone-like apatite on its surface through the formation of calcium-rich amorphous calcium phosphate (ACP) in the early soaking period [30]. It could be inferred from the results that similar event is occurring on surface phosphorylated poly(HEMA-co-MMA). The trend of linear increase in the amount of calcium in the hydroxyapatite coating with time is according to expectation. Varma et al. have reported similar observation for tetra ethoxysilane treated cotton and for phosphorylated chitosan [5, 8]. The possibility of heterogeneous nucleation is significantly high as medium for

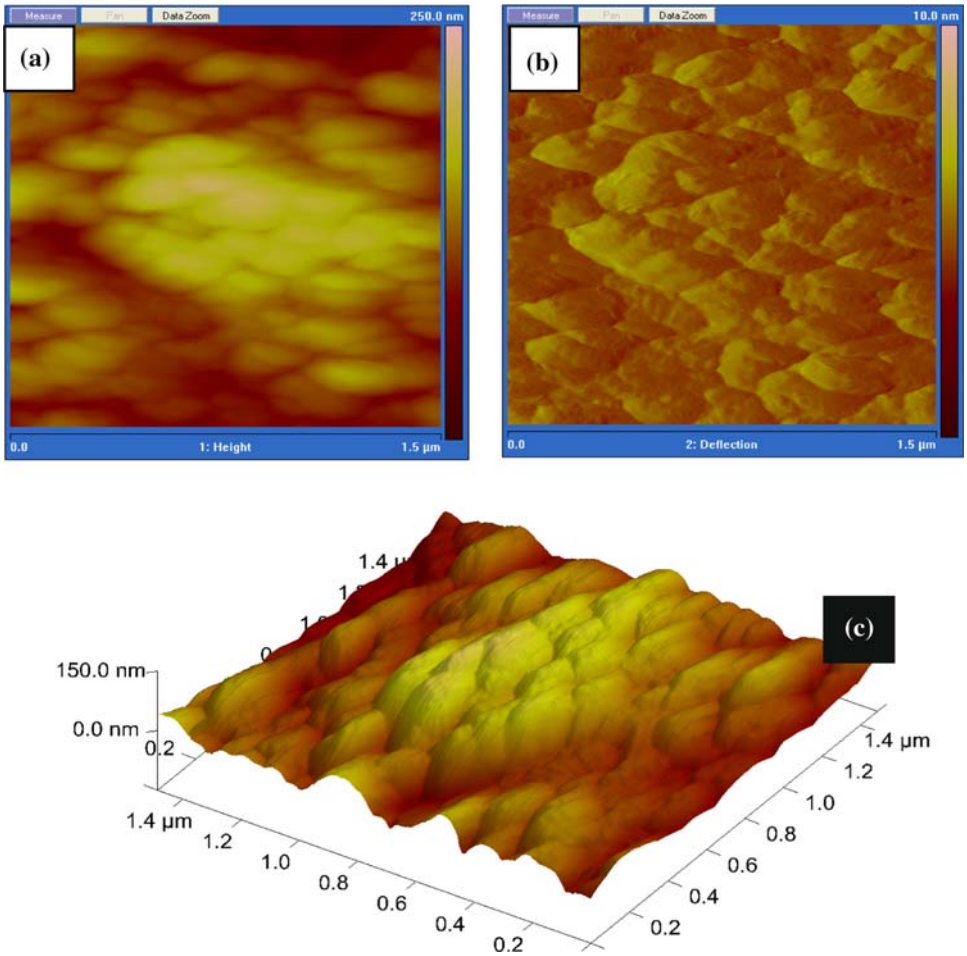

Fig. 7 AFM image of the calcium phosphate coating formed on PPH1 after 3 days immersion in SBF (**a**) height (**b**) deflection (**c**) 3d image

mineralization used is accelerated physiological medium at a high supersaturation.

The calcium concentration of the coating formed on phosphorylated poly(HEMA-co-MMA) increases with increase in HEMA content in phosphorylated PH1 in a linear profile from 10 wt% HEMA towards poly(HEMA) (Fig. 8b). This indirectly relates that the extent of phosphorylation is directly proportional to HEMA content in the copolymer. The linear increase in the amount of phosphate in the phosphorylated copolymer with increase in the wt% of HEMA is basically due to the significantly high concentration of exposed –OH group that could be easily phosphorylated.

Table 2 The calcium concentration in the calcium phosphate coating as a function of HEMA wt% in phosphorylated poly(HEMA-co-MMA) and in phosphorylated poly(HEMA)

Sample code	Wt% of HEMA in the calcium phosphate coated poly(HEMA-co-MMA) series and poly(HEMA)	Calcium concentration in the calcium phosphate coating (µmols/cm^2)
CaPPH1	10	0.5522
CaPPH2	25	2.6799
CaPPH3	50	3.2627
CaPPH4	75	3.7166
CaPPH	100	
Ca(Poly(HEMA)		7.4331

Another main difference between chemical and biological crystallization is the rate of precipitation. Usually in chemical reactions, precipitation occurs fast whereas in biological reactions the crystals need days, weeks, or months to grow [31]. A suitable simulation of this process, especially in the presence of (bio)organic additives, may slow down the crystallization [32]. From the foregoing discussion it could be concluded that the hydroxyapatite nucleation on phosphorylated poly(HEMA-co-MMA) occurs due to the presence of surface bound phosphate groups. Consequently, the number of phosphate group is proportional to the degree of nucleation of hydroxyapatite on the surface of phosphorylated PH1. The study thus imparts significant information on the potential of surface phosphorylated poly(2-hydroxy ethyl methacrylate-co-methyl methacrylate) to invoke bioinspired mineralization

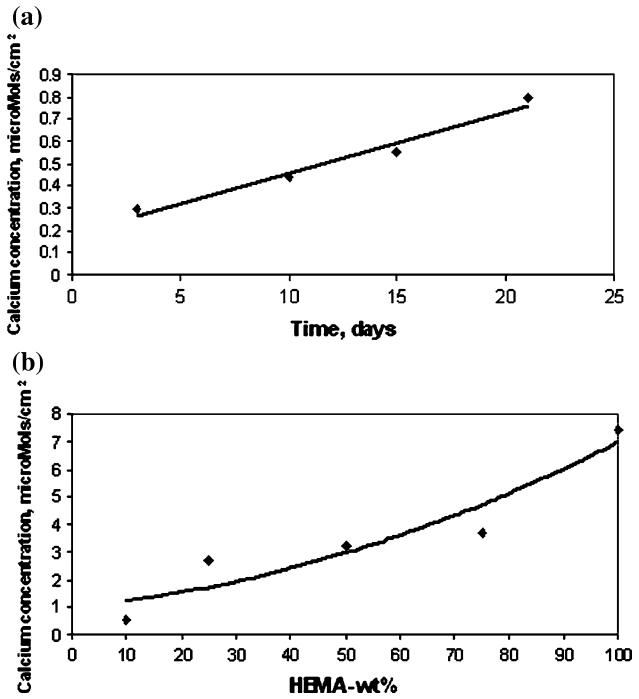

Fig. 8 **a** Calcium concentration of the mineralized coating formed on PPH1 as a function of time. **b** The calcium concentration in the coating after 15 days in SBF as a function of HEMA-wt% in poly(HEMA-co-MMA)

of calcium phosphate. The results of ultrastructural study also illustrate that the transformation of primary nuclei of amorphous calcium phosphate phase to crystalline phase begins within 3 days of immersion in SBF.

5 Conclusions

The surface phosphorylated poly(HEMA-co-MMA) induces bioinspired mineralization of calcium phosphate phase. The surface phosphorylation is proportional to the HEMA content (wt%). The calcium phosphate phase formed is distinctly hydroxyapatite. The ultra-structural analysis shows that the primary nuclei of calcium phosphate transforms to needle like calcium rich apatite crystals within 3 days immersion in SBF and the crystals grow in the c-axis. The concentration of calcium in the coating increases with increase in HEMA content in the copolymer and hence the surface phosphorylated poly(HEMA-co-MMA) could be proposed as a potential substrate capable of eliciting in vitro mineralization of hydroxyapatite.

Acknowledgement G.S. Sailaja expresses gratitude to Council of Scientific and Industrial Research (CSIR, New Delhi, India) for Senior Research Fellowship.

References

1. Hoffman AS. In: Ratner BD, Hoffman AS, Lemons FJ, editors. Biomaterials science: an introduction to materials in medicine. New York: Academic Press; 1996. p. 124. Chap 2.
2. Goissis G, Maginador SVS, da Conceição Amaro Martins V. Biomimetic mineralization of charged collagen matrices: in vitro and in vivo study. Artif Organs. 2003;27(5):437–43.
3. Chen Y, Mark AFT, Wang M, Li J. Composite coating of bonelike apatite particles and collagen fibres on poly(L-Lactic acid) formed through an accelerated biomimetic coprecipitation process. J Biomed Mater Res B Appl Biomater. 2006;77B:315–22.
4. Bigi A, Bracci B, Cojazzi G, Panzavolta S, Rubini K. J Biomater Sci Polymer Edn. 2004;15(3):243–54.
5. Varma HK, Yokogawa Y, Espinosa EF, Kawamoto Y, Nishizawa K, Nagata F, et al. In-vitro calcium phosphate growth over functionalized cotton fibers. J Mater Sci Mat Med. 1999;10:395–400.
6. Li S, Liu Q, de Wijn J, Wolke J, Zhou B, de Groot K. In-vitro apatite formation on phosphorylated bamboo. J Mater Sci Mater Med. 1997;8:543–49.
7. Sailaja GS, Sreenivasan K, Yokogawa Y, Kumary TV, Varma HK. Bioinspired mineralization and cell adhesion on surface functionalized poly(vinyl alcohol) films. Acta Biomater. 2009; 5(5):1647–55.
8. Varma HK, Yokogawa Y, Espinosa EF, Kawamoto Y, Nishizawa K, Nagata F, et al. Porous calcium phosphate coating over phosphorylated chitosan film by a biomimetic method. Biomaterials. 1999;20:879–84.
9. Dalas E, Chrissanthopoulos A. The overgrowth of hydroxyapatite on new functionalized polymer. J Cryst Growth. 2003;255:163–69.
10. Tanahashi M, Matsuda T. Surface functional group dependence on apatite formation on self-assembled monolayers in a simulated body fluid. J Biomed Mater Res. 1997;34:305–15.
11. Hendriksa JGE, van Hornb JR, van der Meia HC, Busschera HJ. Backgrounds of antibiotic-loaded bone cement and prosthesis-related infection. Biomaterials. 2004;25:545–56.
12. Nguyen NC, Maloney WJ, Dauskardt RH. Reliability of PMMA bone cement fixation: fracture and fatigue crack-growth behaviour. J Mat Sci Mat Med. 1997;8:8–12.
13. Chaplin RPS, Lee AJC, Hooper RM, Clarke M. The mechanical properties of recovered PMMA bone cement: a preliminary study. J Mat Sci Mat Med. 2006;17(12):1433–48.
14. Mousa WF, Kobayashi M, Shinzato S, Kamimura M, Neo M, Yoshihara S, et al. Biological and mechanical properties of PMMA-based bioactive bone cements. Biomaterials. 2000;21: 2137–46.
15. Kim SB, Kim YJ, Yoon TL, Park SA, Cho IH, Kim EJ, et al. The characteristics of a hydroxyapatite-chitosan-PMMA bone cement. Biomaterials. 2004;25(26):5715–23.
16. Ohtsuki C, Miyazaki T, Kyomoto M, Tanihara M, Osaka A. Development of bioactive PMMA-based cement by modification with alkoxysilane and calcium salt. J Mat Sci Mat Med. 2001;12: 895–99.
17. Varma HK, Sreenivasan K, Yokogawa Y, Hosumi A. In vitro calcium phosphate growth over surface functionalised PMMA film. Biomaterials. 2003;24:297–303.
18. Kwon SY, Kim YS, Woo YK, Kim SS, Park JB. Hydroxyapatite impregnated bone cement: in vitro and in vivo studies. Biomed Mater Eng. 1997;7(2):129–40.
19. Sailaja GS, Mohanty M, Mohanan PV, Kumary TV, Ramesh P, Varma HK. Surface phosphorylated copolymer promotes direct bone bonding. Tissue Engineering. 2009;15(10):3061–9.

20. Ferrel RE, Olcott HS, Fraenkel-Conrat H. Phopshorylation of proteins with phosphoric acid containing excess phosphorous pentoxide. J Am Chem Soc. 1948;2101–4.
21. Strickland JDH, Parsons TR. Determination of reactive phosphorus. In: A practical handbook of seawater analysis. Fish Res Board Canada Bull. 1968;167:49–56.
22. Kokubo T, Ito S, Huang ZT, Hayshi T, Sakka S, Kitsugi T. Ca, P-rich layer formed on high strength bioactive glass ceramic A-W. J Biomed Mater Res. 1990;24(3):331–43.
23. Ratner BD, Weathersby PK, Hoffman AS, Kelly MA, Scharpen LH. Radiation-grafted hydrogels for biomaterial applications as studied by the ESCA technique. J Appl Polym Sci. 1978;22(3): 643–64.
24. Zhu P, Masuda Y, Koumoto K. The effect of surface charge on hydroxyapatite nucleation. Biomaterials. 2004;25(17):3915–21.
25. Mann S. Biomineralization and biomimetic materials chemistry. In: Biomimetic materials chemistry. New York: VCH Publishers; 1996. p. 14–5.
26. Moreno EC, Gregory TM, Brown WE. Preparation and solubility of hydroxyapatite. J Res Natl Bur Stand. 1968;72A:773–82.
27. Blumenthal NC, Posner AS. Hydroxyapatite: mechanism of formation and properties. Calcif Tissue Res. 1973;13:235–43.
28. Eanes ED. The interaction of supersaturated calcium phosphate solutions with apatitic substrates. Calcif Tissue Res. 1976;20:75–89.
29. Hunter GK, Goldberg HA. Modulation of crystal formation by bone phosphoproteins: role of glutamic acid-rich sequences in the nucleation of hydroxyapatite by bone sialoprotein. Biochem J. 1994;302:175–79.
30. Kim HM, Himeno T, Kawashita M, Kokubo T, Nakamura T. The mechanism of biomineralization of bone-like apatite on synthetic hydroxypatite: an in vitro assessment. J R Soc Interface. 2004; 1:17–22.
31. Nancollas GH. The involvement of calcium phosphates in biological mineralization and demineralization processes. Pure Appl Chem. 1992;64(11):1673–78.
32. Aksay IA, Trau M, Manne S, Honma I, Yao N, Zhou L. Biomimetic pathways for assembling inorganic thin films. Science. 1996;273:892–8.